

ORIGINAL ARTICLE

NAFLD exacerbates cholangitis and promotes cholangiocellular carcinoma in mice

Shin Maeda¹  | Yohko Hikiba¹ | Hiroaki Fujiwara² | Tsuneo Ikenoue³ | Soichiro Sue¹ | Makoto Sugimori¹ | Mao Matsubayashi¹ | Hiroaki Kaneko¹ | Kuniyasu Irie¹ | Tomohiko Sasaki¹ | Makoto Chuma⁴

¹Department of Gastroenterology, Yokohama City University Graduate School of Medicine, Yokohama, Japan

²Division of Gastroenterology, Institute for Adult Diseases, Asahi Life Foundation, Tokyo, Japan

³Division of Clinical Genome Research, Advanced Clinical Research Center, The Institute of Medical Science, The University of Tokyo, Tokyo, Japan

⁴Gastroenterological Center, Yokohama City University Medical Center, Yokohama, Japan

Correspondence

Shin Maeda, Department of Gastroenterology, Yokohama City University Graduate School of Medicine, Yokohama, Japan.

Email: smaeda@yokohama-cu.ac.jp

Funding information

Ministry of Education, Culture, Sports, Science, and Technology of Japan, Grant/Award Number: #19K08373 and #19K34567

Abstract

Nonalcoholic fatty liver disease (NAFLD) is an increasingly common condition, affecting up to 25% of the population worldwide. NAFLD has been linked to several conditions, including hepatic inflammation, fibrosis, and hepatocellular carcinoma (HCC), however the role of NAFLD in cholangitis and the development of cholangiocellular carcinoma (CCC) remains poorly understood. This study investigated whether a high-fat diet (HFD) promotes cholangitis and the development of CCC in mice. We used liver-specific E-cadherin gene (*CDH1*) knockout mice, *CDH1*^{ΔLiv}, which develop spontaneous inflammation in the portal areas along with periductal onion skin-like fibrosis, similar to that of primary sclerosing cholangitis (PSC). An HFD or normal diet (ND) was fed to *CDH1*^{ΔLiv} mice for 7 mo. In addition, *CDH1*^{ΔLiv} mice were crossed with *LSL-Kras*^{G12D} mice, fed an HFD, and assessed in terms of liver tumor development. The extent of cholangitis and number of bile ductules significantly increased in mice fed an HFD compared with ND-administered *CDH1*^{ΔLiv} mice. The numbers of Sox9 and CD44-positive stem cell-like cells were significantly increased in HFD mice. *LSL-Kras*^{G12D}/*CDH1*^{ΔLiv} HFD mice exhibited increased aggressiveness along with the development of numerous HCC and CCC, whereas *LSL-Kras*^{G12D}/*CDH1*^{ΔLiv} ND mice showed several macroscopic tumors with both HCC and CCC components. In conclusion, NAFLD exacerbates cholangitis and promotes the development of both HCC and CCC in mice.

KEYWORDS

carcinoma, cholangitis, steatohepatitis

1 | INTRODUCTION

Nonalcoholic fatty liver disease (NAFLD) is becoming increasingly common, due in part to the wide spectrum of disease pathologies, ranging from simple liver fat deposition to more severe presentations such as nonalcoholic steatohepatitis (NASH), liver cirrhosis

(LC), and hepatocellular carcinoma (HCC). It is estimated that 25% of the world's population has NAFLD.¹ The etiology of the disease is related to diet, body mass index, gut microbiota, and genetic factors.²

Liver cancer is one of the major types of cancer-related death worldwide.³ Common forms include HCC and cholangiocellular

This is an open access article under the terms of the Creative Commons Attribution-NonCommercial License, which permits use, distribution and reproduction in any medium, provided the original work is properly cited and is not used for commercial purposes.

© 2021 The Authors. Cancer Science published by John Wiley & Sons Australia, Ltd on behalf of Japanese Cancer Association.

carcinoma (CCC), which can sometimes present as mixed type carcinomas. The prognosis of patients with liver cancer has improved recently due to advances in diagnosis and treatment; however, the long-term prognosis remains unsatisfactory.⁴ A greater understanding of the molecular mechanisms underlying liver carcinogenesis is therefore needed to address these shortcomings.

Recent evidence has suggested that NAFLD with fibrosis or cirrhosis increases the risk of developing HCC.⁵ Such an association is consistent with recent studies suggesting that between 4% to 22% of HCC cases may be related to NAFLD.⁵ Another type of liver cancer, CCC, arises from various cell types within the biliary tree. There are several major risk factors for the development of CCC, including primary sclerosing cholangitis (PSC), viral infection (hepatitis B virus [HBV] and hepatitis C virus [HCV]), LC, and biliary stone disease.⁶ Metabolic conditions including diabetes and obesity have also been identified as risk factors for CCC.⁷

Recent studies have reported several mechanisms, such as the epithelial-mesenchymal transition (EMT), which may promote carcinogenesis.⁸ Mutation or decreased expression of E-cadherin is associated with malignant progression of various cancers, including HCC and CCC.^{9,10} As deletion of E-cadherin is known to promote invasiveness and EMT, liver-specific knockout of E-cadherin has been used as a model for examining tumor progression in the liver.¹¹ Furthermore, liver-specific deletion of E-cadherin was shown to induce spontaneous periportal inflammation resembling PSC, indicating that these mice can also be used as a model of cholangitis.

Nonalcoholic fatty liver disease is associated with several important comorbidities, including hepatic inflammation, fibrosis, and the development of HCC, however the role of NAFLD in cholangitis and the development of CCC remains poorly understood. This study investigated whether HFD promotes cholangitis and the development of CCC in mice.

2 | MATERIALS AND METHODS

2.1 | Animals

CDH1^{F/F}, *Alb-Cre*, *Alb-CreERT*, *CK19-CreERT*, *Kras^{LSLG12D}*, and *Rosa26^{tdTomato}* mice were purchased from the Jackson Laboratory (Bar Harbor, MN, USA). All knockout strains were developed on the C57BL/6 genetic background. Mice were maintained in filter-topped cages on autoclaved food and water at Yokohama City University. All animal experiments were approved by the Ethics Committee for Animal Experimentation of Yokohama City University and conducted in accordance with the Guidelines for the Care and Use of Laboratory Animals.

2.2 | Reagents

The following antibodies were used in the experiments: anti-CD44 (AbD Serotec); anti-Sox9 and anti-K19 (Santa Cruz Biotechnology),

anti-F4/80 (Caltag), anti-Ki67 (Gene Tex), anti-HNF4 α (Abcam), and anti-RFP (Rockland).

2.3 | High-fat diet

Mice were fed with a normal or high-fat diet (HFD) (40% kcal fat [22% trans-fat and 26% saturated fatty acids by weight], 22% fructose, 10% sucrose, 2% cholesterol; D09100301, Research Diets).

2.4 | Immunohistochemical analyses

Liver tissue was fixed in 10% formaldehyde, dehydrated, embedded in paraffin, and sectioned (5 μ m thickness). Sections were deparaffinized, rehydrated, treated with 3% H₂O₂ in PBS, and incubated overnight at 4°C with the appropriate antibodies. Binding of the primary antibody was detected using biotin-labeled anti-rabbit IgG or anti-rat IgG antibodies (1:500 dilution; Vector Laboratories), followed by the streptavidin-horseradish peroxidase (HRP) reaction and visualization with 3,3-diaminobenzidine (DAB; Sigma) and counterstaining with hematoxylin. For the double staining, sections were incubated with 1st primary antibody (1:500) overnight at 4°C, and the immunoreactivity was visualized with DAB (brown staining) with a peroxidase-based Histofine Simple Stain Kit (MAX PO R, Nichirei). For the immunoreactivity to another target, 2nd primary anti (1:500) was incubated overnight at 4°C and visualized with Fast Red II Substrate (Nichirei) using an alkaline phosphatase-based Histofine Simple Stain Kit (AP R, Nichirei).

2.5 | Statistical analysis

Data are expressed as the mean \pm standard error of the mean (SEM). Significant differences were determined using Student *t* test. *P*-values \leq .05 were considered significant.

3 | RESULTS

3.1 | NAFLD exacerbates cholangitis caused by E-cadherin deletion

Previously, we have shown that liver-specific E-cadherin knockout mice (*CDH1^{ΔL}*) developed spontaneous periportal inflammation as well as periductal fibrosis, which resembles PSC. To determine the role of NAFLD in cholangitis, *CDH1^{ΔL}* mice were fed an HFD for 20 wk to induce NAFLD. *CDH1^{ΔL}* mice fed the HFD exhibited significant increases in body weight and fat deposition, similar to HFD-administered *CDH1^{F/F}* control mice (Figure 1A,B, Figure S1). HFD-administered *CDH1^{ΔL}* mice exhibited steatosis, ballooning, and inflammation similar to that of *CDH1^{F/F}* mice, and the cholangitis in the periportal area was more severe compared with that seen in mice fed a ND (Figure 1B and Figure S1). To better assess the inflammatory

response, we performed immunostaining of F4/80 myeloid cells in $CDH1^{\Delta L}$ mice, and observed a significant increase in the number of F4/80-positive cells in the periportal area of mice fed an HFD relative to ND controls (Figure 1C). CD45- and CD3-positive lymphoid cells were also increased in HFD mice, although the overall number of CD45-positive cells was relatively small compared with F4/80 myeloid cells (data not shown). We observed increased ALT expression in both $CDH1^{\Delta L}$ and $CDH1^{F/F}$ control mice fed the HFD, with no significant difference between strains. Serum levels of total alkaline phosphatase (ALP) and bile acid were increased in $CDH1^{\Delta L}$ mice compared with $CDH1^{F/F}$ control mice, however the ALP and total bile acid levels were not different between ND and HFD mice (Figure 1D).

$CDH1^{\Delta L}$ showed numerous primitive duct cells expressing progenitor markers, such as Sox9 and CD44, in the periportal area.¹¹ $CDH1^{\Delta L}$ HFD mice showed increased numbers of Sox9- and CD44-positive cells compared with ND mice (Figure 2A,B). CK19-positive ductular cells were also increased by HFD (Figure 2A,B). Interestingly, Sox9-positive cells were observed not only in zone 1, but also in zone 2 of $CDH1^{\Delta L}$ HFD mice compared with only zone 1 in the $CDH1^{\Delta L}$ ND mice (Figure 2A,B). $CDH1^{F/F}$ HFD mice showed slightly but not significantly increased numbers of Sox9, CD44 and CK19-positive cells compared with ND mice (Figure S2). We performed double staining of Sox9/CK19 and Sox9/CD44 (Figure 2B), and found that Sox9 and CK19 were stained in almost the same cells. Most of the

Sox9-positive cells were positive for CD44, however CD44 single positive cells were frequently found, possibly because of the positivity of CD44 in mesenchymal cells in addition to immature cholangiocytes. In contrast, $CDH1^{F/F}$ HFD mice showed slightly, but not significantly, increased numbers of Sox9-, CD44-, and CK19-positive cells (Figure 2C). These results suggested a significant increase in the extent of cholangitis and the number of bile ductules in $CDH1^{\Delta L}$ HFD mice relative to $CDH1^{\Delta L}$ ND mice. Fibrosis, as determined using α -smooth muscle actin (α -SMA) immunostaining, was slightly increased in $CDH1^{\Delta L}$ HFD mice relative to ND controls (data not shown).

3.2 | The NAFLD-induced exacerbated ductular reaction might be irreversible

To determine whether the ductular reaction seen in these mice is reversible, mice fed the HFD diet for 5 mo were switched to the ND for 3 wk. We found that severe cholangitis and fat deposition in $CDH1^{\Delta L}$ were significantly reversed after 3 wk; however, the increased ductular reaction, as well as the increased numbers of Sox9, CD44 and CK19-positive cells were not reversed (Figure 3A,B). In contrast, the number of F4/80 myeloid cells was reduced in these mice (Figure 3C), suggesting that the NAFLD-induced bile duct reaction may be irreversible over short time periods.

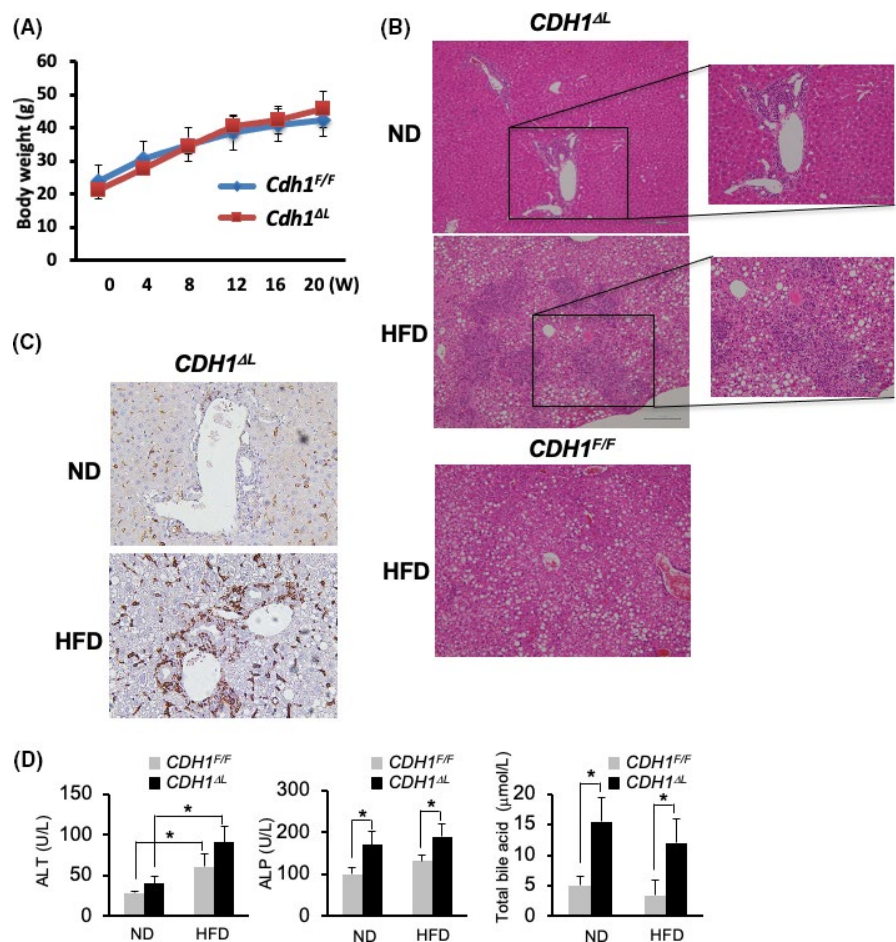
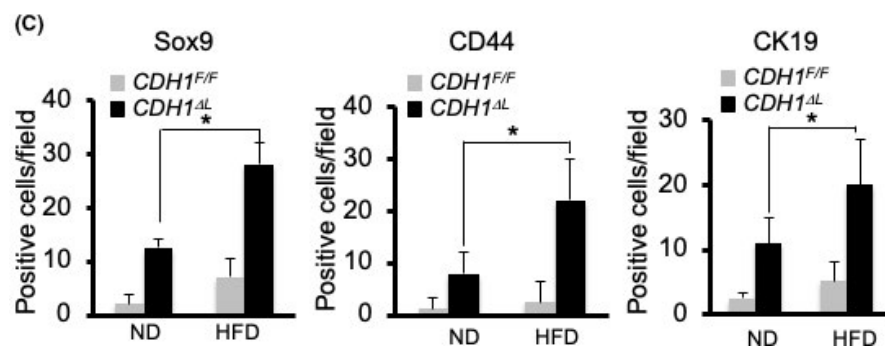
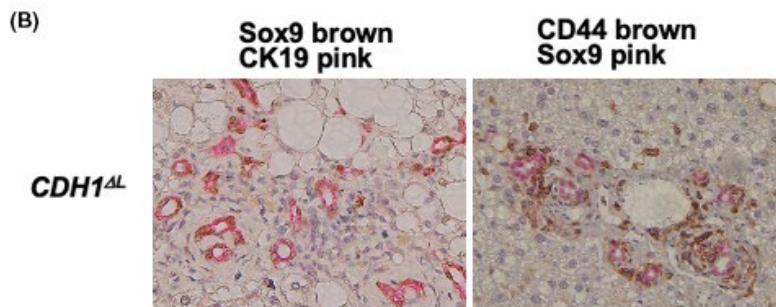
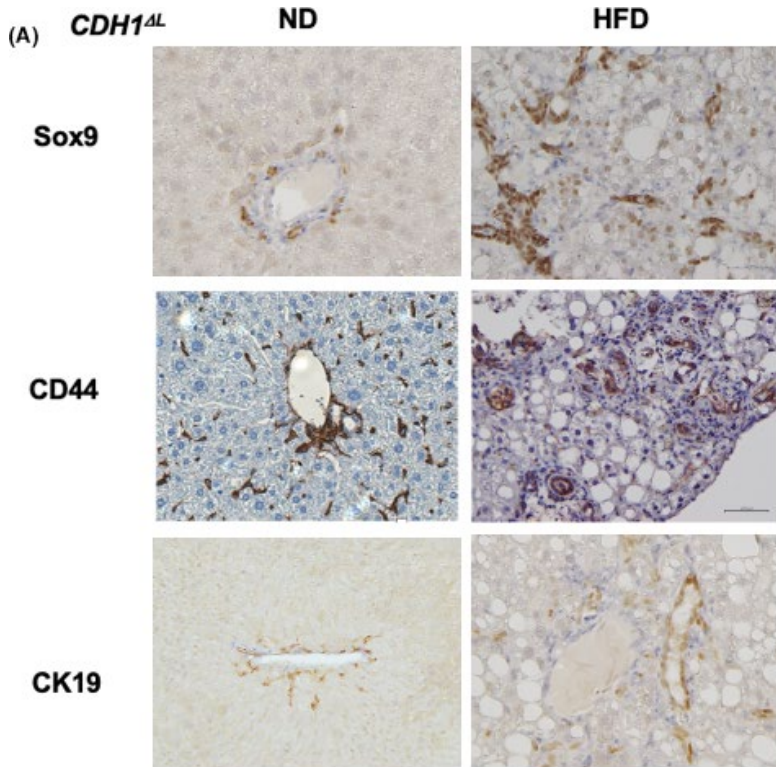


FIGURE 1 NAFLD exacerbates cholangitis caused by E-cadherin deletion. A, Body weight curve of $CDH1^{\Delta L}$ mice ($n = 5$) and $CDH1^{F/F}$ ($n = 5$) after HFD. B, H&E staining of the liver in ND and HFD $CDH1^{\Delta L}$ mice and $CDH1^{F/F}$ HFD mice. $\times 100$ (left panel) and $\times 200$ (right panel) magnification. C, Immunostaining of F4/80 in $CDH1^{\Delta L}$ ND and HFD mice. $\times 200$ magnification. D, Serum ALT, ALP, and total bile acid levels of ND and HFD mice of each genotype (both $n = 5$). Values represent the mean \pm standard error of the mean (SEM). * $P < .05$ as determined by Student t test



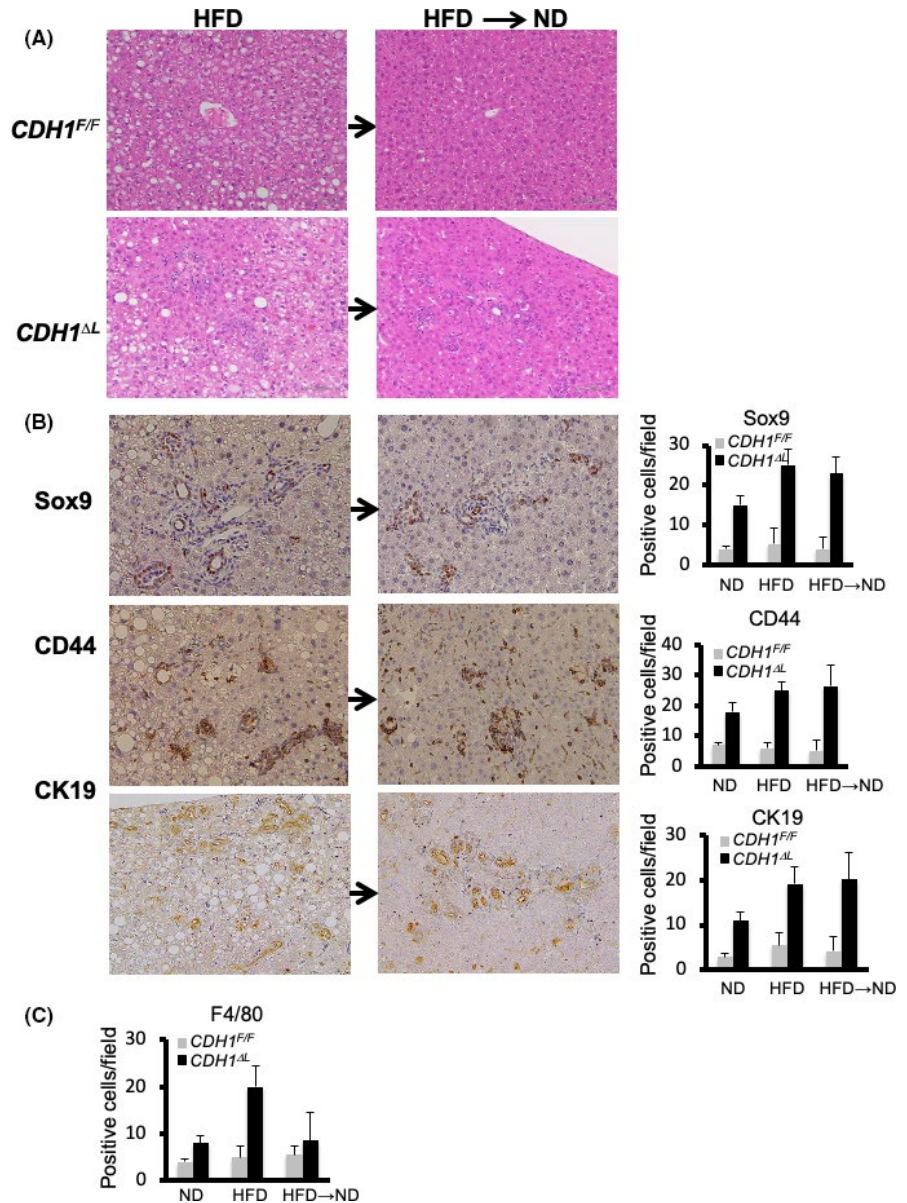
3.3 | Increased ductular reaction induced by HFD may be due to bile duct epithelial cells

We have previously reported that loss of E-cadherin in bile duct epithelial cells (BECs) rather than hepatocytes induces cholangitis and ductular reaction in *CDH1^{ΔL}*.¹¹ We also showed that E-cadherin was deleted both in hepatocytes and BECs of *CDH1^{ΔL}* mice.¹¹ Therefore, we wanted to determine whether the increased ductular reaction

FIGURE 2 NAFLD increased Sox9-, CD44-, and CK19-positive cells in E-cadherin-deleted liver. A, Immunostaining of Sox9, CD44, and CK19 in *CDH1^{ΔL}* ND and HFD mice (×200 magnification). B, Double immunostaining of Sox9 (brown)/CK19 (pink) (left panel) and CD44 (brown)/Sox9 (pink) (right panel) in *CDH1^{ΔL}* HFD mice (×200 magnification). C, Quantification of Sox9, CD44, and CK19 cells in *CDH1^{ΔL}* (n = 5) and *CDH1^{F/F}* (n = 5) mice. Positive cell numbers per field. *P < .05

associated with HFD was also associated with BECs. To delete E-cadherin only in BECs, we crossed *CDH1^{F/F}* mice with *K19CreERT* mice expressing a tamoxifen (TAM)-inducible Cre ERT in the endogenous *K19* locus (*CDH1^{F/F}/K19CreERT; CDH1^{Δich}*) (Figure 4A). At 12 wk after TAM injection, increased cholangitis (F4/80-positive cells), ductular reaction (CK19-positive), and Sox9-positive staining were observed in ND mice, as described previously¹¹ (Figure 4B). In *CDH1^{Δich}* mice, HFD increased cholangitis (F4/80-positive cells), ductular reactivity

FIGURE 3 NAFLD-induced exacerbation of the ductular reaction may be irreversible. A, H&E staining of $CDH1^{\Delta L}$ ($n = 4$) and $CDH1^{F/F}$ ($n = 4$) mice fed an HFD for 5 mo before being switched to ND for 3 wk. B, Sox9, CD44, and CK19 immunostaining and quantification. $\times 200$ magnification. C, Quantification of F4/80-positive cells



(CK19-positive cells), and Sox9-positive staining compared with ND mice (Figure 4B,C). These observations suggested that the increased cholangitis and ductular reactivity induced by HFD were dependent on BECs (Figure 4A–C). However, compared with $CDH1^{\Delta L}$ HFD mice, CK19- and Sox9-positive cell expression in $CDH1^{\Delta L}$ HFD mice was relatively limited around zone 1. To confirm that the increased ductular reaction was derived from E-cadherin-deleted BECs, we crossed $Rosa26^{tdTomato}$ mice ($tdTomato$ mice) with $CDH1^{\Delta L}$ mice and found that most of the ductular cells were $tdTomato$ -positive, suggesting that the increase in ductular cells was derived from CK19-positive BECs in HFD-administered $CDH1^{\Delta L}$ mice (Figure 4D).

3.4 | Increased primitive cell expression induced by HFD was also due to hepatocytes

Biphenotypic hepatocytes, also known as ductular hepatocytes, express ductal markers and give rise to ductal cells, and have been

reported in cholestatic liver injury models.^{12–14} Furthermore, pre-existing populations of Sox9-expressing periportal hepatocytes and other bile-duct-enriched genes have shown extensive proliferation after chronic injuries.¹⁵ In $CDH1^{\Delta L}$ mice, an HFD increased Sox9-positive cells, not only in zone 1, but also in zone 2 (Figure 2A). Therefore, we wanted to determine whether hepatocytes other than BECs were the source of Sox9-positive cells. To generate hepatocyte-specific E-cadherin knockout mice, we crossed $CDH1^{F/F}$ mice with $Alb-CreERT$ mice expressing a TAM-inducible Cre ERT in the endogenous albumin locus ($CDH1^{F/F}/Alb-CreERT$; $CDH1^{\Delta hep}$). $CDH1^{\Delta hep}$ and control mice were injected with TAM at 6 wk of age and fed with the HFD or ND for 12 wk (Figure 5A). No obvious phenotype was found in $CDH1^{\Delta hep}$ ND mice, consistent with our previous report of no apparent periportal inflammation associated with the injection of adenovirus-expressing Cre recombinase in $CDH1^{F/F}$ mice.¹¹ Interestingly, $CDH1^{\Delta hep}$ HFD mice showed increased numbers of small Sox9-positive hepatocyte-like cells, with no such phenotype seen in control HFD mice (Figure 5B–D). As shown in

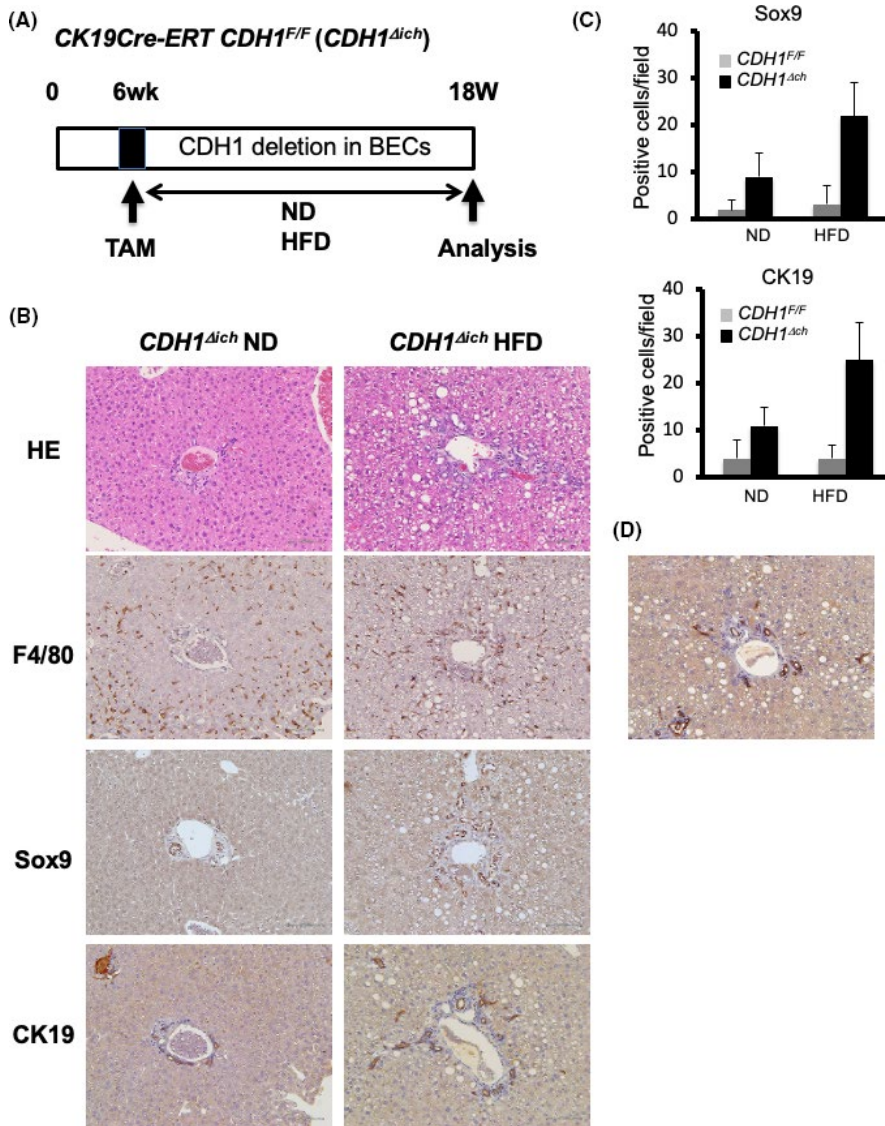


FIGURE 4 Increased ductular reaction induced by the HFD may be due to bile duct epithelial cells. A, $CDH1^{F/F}$ mice crossed with $K19CreERT$ mice, in which a TAM-inducible CreERT was inserted into the endogenous $K19$ locus ($CDH1^{F/F}/K19CreERT;CDH1^{\Delta ich}$). B, At 12 wk after TAM injection, mice were fed with a ND or HFD. H&E and immunostaining results of F4/80, Sox9, and CK19 are shown ($\times 100$ magnification). C, Quantification of Sox9- and CK19-positive cells of $CDH1^{F/F}$ and $CDH1^{\Delta ich}$ mice fed the ND or HFD are shown ($n = 5$ for all groups). D, $Rosa26^{tdTomato}$ mice were crossed with $CDH1^{\Delta ich}$ mice; most of the ductular cells were tdTomato-positive, suggesting that increased ductular cell expression in HFD-administered mice was due to BECs ($\times 100$ magnification)

Figure 5C, Sox-9 cells were located in both zone 1 and zone 2. CK19-positive cells were slightly increased in $CDH1^{\Delta hep}$ HFD mice relative to both $CDH1^{\Delta hep}$ ND and $CDH1^{F/F}$ HFD mice.

To determine the source of the Sox9-positive cells in $CDH1^{\Delta hep}$ HFD mice, these mice were crossed with tdTomato mice, as described above. We found that the Sox9-positive cells in zone 2 were derived from Alb-positive hepatocytes. These observations indicated that E-cadherin deletion in hepatocytes led to the production of hepatoblast-like cells by steatosis. These results suggested that increased Sox9-positive cell expression in $CDH1^{\Delta hep}$ was due to both hepatocytes and BECs.

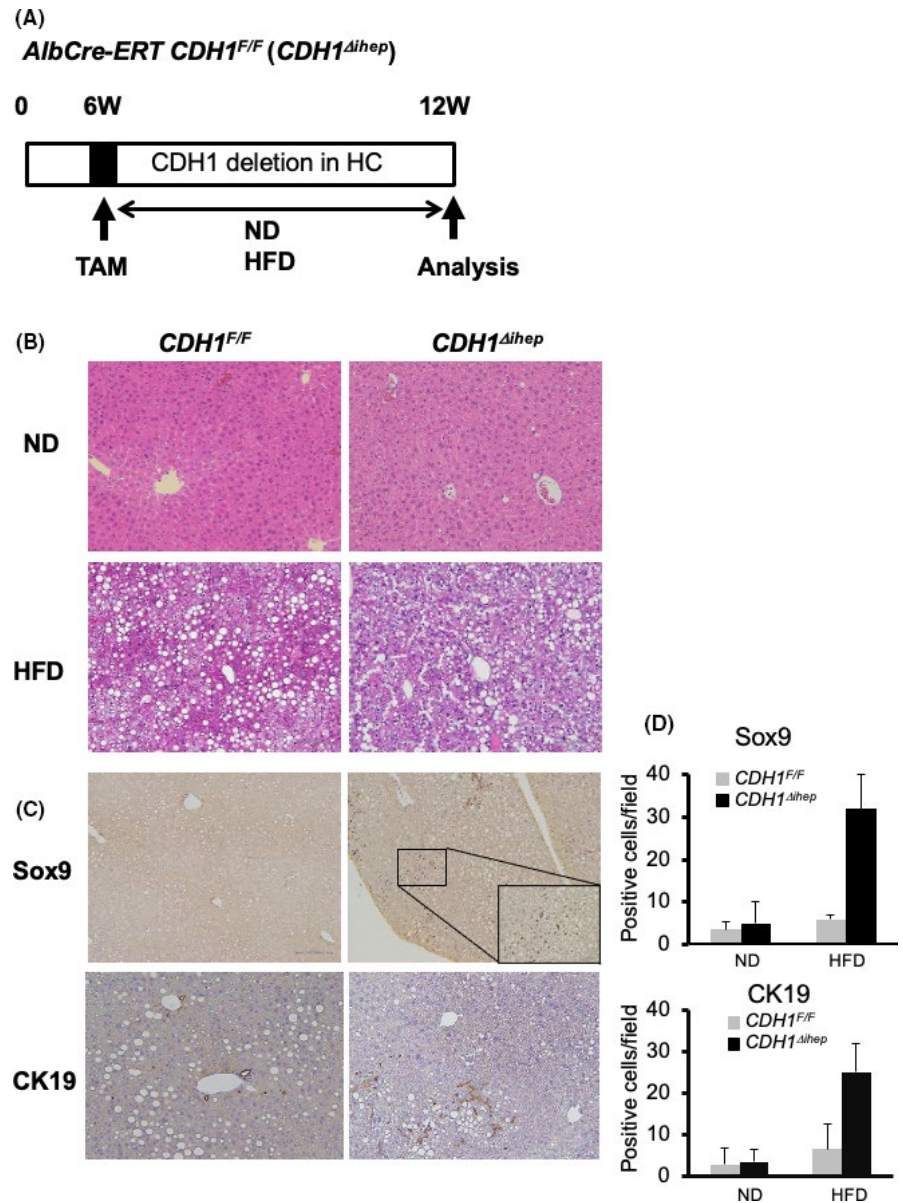
3.5 | High-fat diet promotes tumorigenesis in $CDH1^{\Delta L}$

Previously, we showed that a small percentage of male $CDH1^{\Delta L}$ mice (2/12, 16.7%) spontaneously developed liver tumors by 11 mo of age.¹¹ In this study, we analyzed tumorigenesis in

8-mo-old $CDH1^{\Delta L}$ HFD mice over 6 mo. The overall tumor incidence was 2/11 (22.2%), representing a small, but noticeable, difference compared with $CDH1^{\Delta L}$ ND mice (0/8; 0%). The majority of the tumors in the $CDH1^{\Delta L}$ HFD mice contained both hepatocellular and ductular (cholangiocellular) components (Figure 6A, left panel); the others contained only ductular or hepatocellular component (Figure 6A, right panel). As only 2 $CDH1^{\Delta L}$ HFD mice developed spontaneous tumors, it was difficult to determine whether mixed type, hepatocellular, or cholangiocellular tumors were more common in this group.

As the incidence of tumors in $CDH1^{\Delta L}$ HFD mice was too low to analyze further, we expanded our analysis to tumor incidence in liver-specific *Kras*-expressing mice ($Alb-cre/Kras^{LSLG12D};Kras$). At 5 mo of age, there were no visible tumors in any of the *Kras* ND mice (0/8; 0%). *Kras* mice fed the HFD (starting at 2 mo of age) sacrificed at 5 mo old (3-mo HFD) showed visible white lesions containing histologically confirmed hepatocellular tumors (8/8;10%; Figure 6B,C, right panel). The number of tumor foci was increased in *Kras* HFD mice compared with ND controls (Figure 6D). These

FIGURE 5 HFD-induced Sox9-positive cells were derived from hepatocytes. A, $CDH1^{F/F}$ mice were crossed with $Alb-CreERT$ mice, in which a TAM-inducible CreERT was inserted into the endogenous albumin locus ($CDH1^{F/F}/Alb-CreERT;CDH1^{\Delta hep}$ or control mice were injected with TAM at 6 wk of age and fed a ND or HFD for 12 wk. B, H&E staining of the liver of $CDH1^{F/F}$ and $CDH1^{\Delta hep}$ mice fed the ND or HFD ($\times 100$ magnification). C, Sox9 and CK19 immunostaining in the liver of $CDH1^{F/F}$ and $CDH1^{\Delta hep}$ mice fed the HFD. D, Quantification of Sox9- and CK19-positive cells in $CDH1^{F/F}$ and $CDH1^{\Delta hep}$ mice fed the HFD are shown ($n = 5$ for all groups)



results suggested that *Kras* HFD mice can be used as a model for hepatocarcinogenesis.

To analyze the role of cholangitis in HFD-induced hepatocarcinogenesis, *Kras/CDH1^{ΔL}* mice were transitioned to an HFD at 2 mo and analyzed after 3 mo (5 mo of age). *Kras/CDH1^{ΔL}* ND mice developed a small number of visible liver tumors at 5 mo of age, however the *Kras/CDH1^{ΔL}* HFD group exhibited a significant increase in tumor burden compared with *Kras/CDH1^{+/+}* mice (Figure 6C,D). Histological analyses revealed a variety of tumor types, including cholangiocellular (CC) (34%), cholangiocellular/hepatocellular (Mixed) (42%) and hepatocellular (24%) (HC) tumors (Figure 6F) determined using immunostaining of CK19 for CC and HNF4 α for HC tumors (Figure 6G). These results suggested that loss of E-cadherin exacerbated HFD-related increases in Ras signaling, resulting in enhanced development of both hepatocellular and cholangiocellular tumors.

4 | DISCUSSION

In this study, we observed a significant increase in the extent of cholangitis and fibrosis, and in the number of bile ductules in $CDH1^{\Delta Liv}$ mice fed an HFD for 7 mo compared with ND-administered mice (Figure 7). The numbers of CD44- and Sox9-positive stem cell-like cells were also increased in HFD mice.

Overweight and obese PSC patients have been found to exhibit more advanced fibrosis, as well as more rapid progression of fibrosis, compared with normal weight patients.¹⁶ Several other liver diseases are known to elicit ductular reactions such as chronic viral hepatitis.¹⁷ Therefore, an increased ductular reaction in response to HFD may be more common than previously thought and may be associated with cancer development.

The mechanism by which obesity or NAFLD leads to more aggressive inflammation and an increased ductular reaction is unknown.

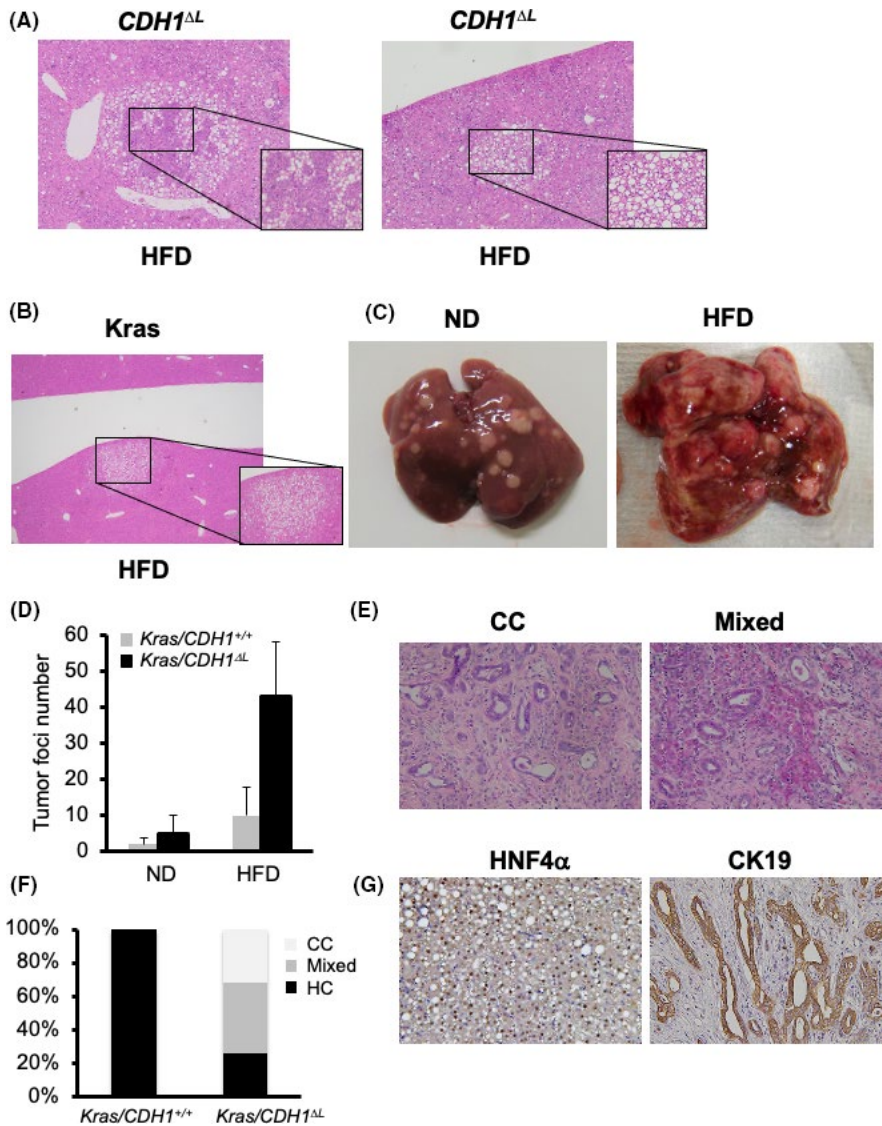


FIGURE 6 High-fat diet promotes tumorigenesis in *CDH1*^{ΔL}. A, Tumors in 8-mo-old *CDH1*^{ΔL} mice fed an HFD for 6 mo (×100 magnification). B, Tumors of Alb-cre/*LSL-Kras*^{G12D} (*Kras*^{hep}) HFD mice. *Kras*^{hep} mice were started on an HFD at 2 mo of age and sacrificed at 5 mo (3-mo HFD). C, Macroscopic features of *Kras*^{hep}/*CDH1*^{F/F} and *Kras*^{hep}/*CDH1*^{ΔL} mice fed the HFD. D, The number of tumor foci in *Kras*^{hep}/*CDH1*^{F/F} (n = 5) and *Kras*^{hep}/*CDH1*^{ΔL} (n = 7) mice fed the HFD for 3 mo, starting at 2 mo of age. E, H&E staining of CC and Mixed tumors of *Kras*^{hep}/*CDH1*^{ΔL} HFD mice (×100 magnification). F, Tumor histology in the tumors of *Kras*^{hep}/*CDH1*^{F/F} and *Kras*^{hep}/*CDH1*^{ΔL} HFD mice. G, HNF4α and CK19 immunostaining in the HC (left panel) and CC (right panel) tumors of *Kras*^{hep}/*CDH1*^{ΔL} HFD mice (×100 magnification)

We have shown that the ductular reaction in response to E-cadherin deletion is dependent on impairment of the intrahepatic biliary network. In this study, we did not observe any increase in the number of tubules in HFD-fed *CDH1*^{F/F} mice, suggesting that HFD itself is not sufficient to induce a ductular reaction. In contrast, *CDH1*^{ΔLiv} showed an increased ductular reaction in response to HFD. Recent reports have suggested that pathogen-associated molecular pattern (PAMP)-sensing receptors, such as Toll-like receptors, and the subsequent expression of cytokines triggered by their activation, are important for increased ductular reaction.^{18,19} PAMPs are known to activate inflammatory cells, such as Kupffer cells and macrophages, in the liver and also induce the production of inflammatory cytokines and growth factors, such as tumor necrosis factor (TNF)-α and interleukin (IL)-6. Although inflammation is an important factor seen in association with ductule formation, the factors driving their proliferation remain poorly understood. We aimed to induce the ductular reaction in TNF-α knockout mice using antibiotics; however, no significant effect was seen (data not shown).

Based on these observations, we aimed to determine whether this enhanced ductular response promoted CCC. We showed that liver-specific *LSL-Kras*^{G12D}/*CDH1*^{ΔLiv} with ND revealed 2-10 macroscopically visible tumors containing both hepatocellular and cholangiocellular components, and HFD administration induced the development of more numerous and aggressive CCCs. To investigate the source of cholangiocellular tumors, we crossed the *CDH1*^{Δich} and *LSL-Kras*^{G12D} mice, and maintained them on an HFD for 3 mo. Small precancerous lesions were found in all mice, suggesting that the cholangiocellular tumors in *Kras*/*CDH1*^{ΔLiv} mice were at least partially due to the increased expression of CK-19-positive ductular cells (Figure S3). The model CK19-CreERT showed relatively low efficiency of knockdown and *CDH1* was expressed in around 70% of the cholangiocytes (Figure S4). We assume that this potentially explains the low number of tumors in the mouse line when crossed with *Kras*. In contrast, a previous mouse model of cholangiocarcinoma, in which hepatocytes and cholangiocytes were labeled with heritable, cell type-specific reporters, found that cholangiocarcinomas were

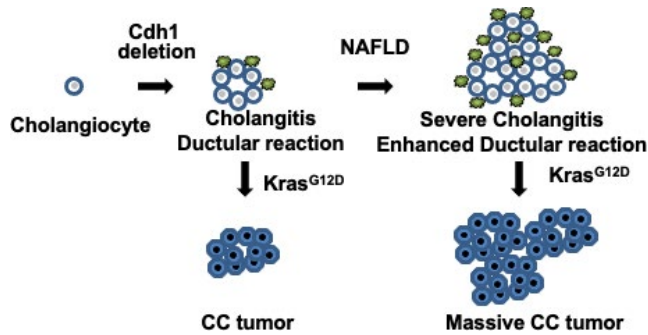


FIGURE 7 Graphic schema of this study. *Cdh1* deletion in cholangiocytes develops spontaneous inflammation (cholangitis) and ductular reaction. The extent of cholangitis and ductular reaction is increased in mice with NAFLD. Additional *Kras* mutation develops cholangiocellular (CC) tumors in mice with *Cdh1* deleted cholangiocytes and NAFLD promotes development of CC tumors

generated by biliary lineage cells derived from hepatocytes, rather than from cholangiocytes.²⁰

In this study, Alb-CreERT/*Kras* (*Kras*^{hep}) mice showed no visible tumors, but histologically small foci were observed in all mice. However, there were more than 10 visible tumors in the *Kras*^{hep}/*CDH1*^{Δhep} HFD mice (Figure 6D). Furthermore, the number of Sox9-positive cells was increased in the background and tumors of *Kras*^{hep}/*CDH1*^{Δhep} mice. To trace these cells, *tdTomato* mice were crossed with *Kras*^{hep}/*CDH1*^{Δhep}. Histological analyses showed that the majority of these cells were Tomato-positive, suggesting that Sox9 positive cells of *Kras*^{hep}/*CDH1*^{Δhep} mice originated from hepatocytes. Most of the tumors were AFP-positive HCC, with only a small proportion of CK19-positive CCC cells. These observations suggested that E-cadherin deleted hepatocytes, which exhibit a Sox9-positive premature NAFLD phenotype, may represent an important source of tumors.

The bile canalicular reaction is caused by the proliferation of liver stem or progenitor cells, such as oval cells. A typical bile duct reaction is characterized by an increase in relatively well-shaped bile ducts with a clear lumen, usually associated with rapid biliary obstruction. Conversely, an atypical bile duct reaction is an irregular form of bile duct hyperplasia often observed in various pathological conditions, such as cirrhosis, alcoholic liver injury, and fulminant hepatitis with inflammation and fibrosis. The atypical bile duct reaction is caused by the proliferation of existing BECs, although the underlying cause of this reaction remains unclear. However, many researchers consider the cause to be the proliferation of stem cells activated by injury, as well as the proliferation of oval cells.

Loss of E-cadherin expression is associated with mutations of the E-cadherin gene *CDH1*, loss of heterozygosity in 16q22.1, or a transcriptional down-regulation of *CDH1* by promoter methylation.^{21,22} Clinically, a decrease or deletion of E-cadherin has been reported in some liver diseases. For example, both HCV and HBV proteins were shown to induce promoter hypermethylation of E-cadherin, resulting in decreased expression and induction of EMT.^{23,24} The presence of hypermethylated E-cadherin in serum has been linked to HCC in patients with HCV-related cirrhosis.²⁵

In summary, NAFLD exacerbates cholangitis and becomes a strong promoter not only of HCC, but also of CCC in mice (Figure 7). As the number of cancer patients with fatty liver continues to rise, a better understanding of the precise molecular mechanisms underlying tumor growth in both normal and NAFLD livers is needed to improve the diagnosis and treatment of these patients.

ACKNOWLEDGMENTS

SM was supported by Grants-in-Aid from the Ministry of Education, Culture, Sports, Science, and Technology of Japan (#19K08373 and #19K34567).

DISCLOSURE

All authors have no competing interests.

ORCID

Shin Maeda  <https://orcid.org/0000-0002-0246-1594>

REFERENCES

1. Araújo AR, Rosso N, Bedogni G, Tiribelli C, Bellentani S Global epidemiology of non-alcoholic fatty liver disease/non-alcoholic steatohepatitis: What we need in the future. *Liver Int.* 2018;38(Suppl. 1):47-51.
2. Buzzetti E, Pinzani M, Tsochatzis EA The multiple-hit pathogenesis of non-alcoholic fatty liver disease (NAFLD). *Metabolism.* 2016;65:1038-1048.
3. Bertuccio P, Alicandro G, Malvezzi M, et al. Cancer mortality in Europe in 2015 and an overview of trends since 1990. *Ann Oncol.* 2019;30:1356-1369.
4. Chew SA, Moscato S, George S, Azimi B, Danti S Liver cancer: Current and future trends using biomaterials. *Cancers (Basel).* 2019;11(12):2026.
5. Younossi ZM, Koenig AB, Abdelatif D, Fazel Y, Henry L, Wymer M Global epidemiology of nonalcoholic fatty liver disease—Meta-analytic assessment of prevalence, incidence, and outcomes. *Hepatology.* 2016;64:73-84.
6. Labib PL, Goodchild G, Pereira SP Molecular pathogenesis of cholangiocarcinoma. *BMC Cancer.* 2019;19:1-16.
7. Petrick JL, Yang B, Altekruse SF, et al. Risk factors for intrahepatic and extrahepatic cholangiocarcinoma in the United States: A population-based study in SEER-Medicare. *PLoS One.* 2017;12:e0186643.
8. Gao D, Vahdat LT, Wong S, Chang JC, Mittal V Microenvironmental regulation of epithelial-mesenchymal transitions in cancer. *Cancer Res.* 2012;72:4883-4889.
9. Terashita K, Chuma M, Hatanaka Y, et al. ZEB1 expression is associated with prognosis of intrahepatic cholangiocarcinoma. *J Clin Pathol.* 2016;69:593-599.
10. Giannelli G, Koudelkova P, Dituri F, Mikulits W Role of epithelial to mesenchymal transition in hepatocellular carcinoma. *J Hepatol.* 2016;65:798-808.
11. Nakagawa H, Hikiba Y, Hirata Y, et al. Loss of liver E-cadherin induces sclerosing cholangitis and promotes carcinogenesis. *Proc Natl Acad Sci.* 2014;111:1090-1095.
12. Tanimizu N, Nishikawa Y, Ichinohe N, Akiyama H, Mitaka T Sry HMG box protein 9-positive (Sox9+) epithelial cell adhesion molecule-negative (EpCAM-) biphenotypic cells derived from hepatocytes are involved in mouse liver regeneration. *J Biol Chem.* 2014;289:7589-7598.
13. Tarlow B, Pelz C, Naugler W, et al. Bipotential adult liver progenitors are derived from chronically injured mature hepatocytes. *Cell Stem Cell.* 2014;15:605-618.

14. Yanger K, Zong Y, Maggs LR, et al. Robust cellular reprogramming occurs spontaneously during liver regeneration. *Genes Dev.* 2013;27:719-724.
15. Font-Burgada J, Shalapour S, Ramaswamy S, et al. Hybrid periportal hepatocytes regenerate the injured liver without giving rise to cancer. *Cell.* 2015;162:766-779.
16. Reyes JL, Vannan DT, Vo T, et al. Neutralization of IL-15 abrogates experimental immune-mediated cholangitis in diet-induced obese mice. *Sci Rep.* 2018;8:1-12.
17. Sato K, Marzioni M, Meng F, Francis H, Glaser S, Alpini G Ductular reaction in liver diseases: pathological mechanisms and translational significances. *Hepatology.* 2019;69:420-430.
18. Odena G, Chen J, Lozano JJ, et al. LPS-TLR4 pathway mediates ductular cell expansion in alcoholic hepatitis. *Sci Rep.* 2016;6:1-15.
19. Joshi-Barve S, Kirpich I, Cave MC, Marsano LS, McClain CJ Alcoholic, nonalcoholic, and toxicant-associated steatohepatitis: Mechanistic similarities and differences. *Cell Mol Gastroentrol Hepatol.* 2015;1:356-367.
20. Sekiya S, Suzuki A Intrahepatic cholangiocarcinoma can arise from Notch-mediated conversion of hepatocytes. *J Clin Invest.* 2012;122:3914-3918.
21. Wang Y, Shang Y Epigenetic control of epithelial-to-mesenchymal transition and cancer metastasis. *Exp Cell Res.* 2013;319:160-169.
22. Fan X, Jin S, Li Y, et al. Genetic and epigenetic regulation of e-cadherin signaling in human hepatocellular carcinoma. *Cancer Manag Res.* 2019;11:8947-8963.
23. Park J, Jang KL Hepatitis C virus represses E-cadherin expression via DNA methylation to induce epithelial to mesenchymal transition in human hepatocytes. *Biochem Biophys Res Commun.* 2014;446:561-567.
24. Arzumanyan A, Friedman T, Kotei E, Ng IOL, Lian Z, Feitelson MA Epigenetic repression of E-cadherin expression by hepatitis B virus x antigen in liver cancer. *Oncogene.* 2012;31:563-572.
25. El-Bendary M, Nour D, Arafa M, Neamatallah M Methylation of tumour suppressor genes RUNX3, RASSF1A and E-Cadherin in HCV-related liver cirrhosis and hepatocellular carcinoma. *Br J Biomed Sci.* 2020;77:35-40.

SUPPORTING INFORMATION

Additional supporting information may be found online in the Supporting Information section.

How to cite this article: Maeda S, Hikiba Y, Fujiwara H, et al. NAFLD exacerbates cholangitis and promotes cholangiocellular carcinoma in mice. *Cancer Sci.* 2021;112: 1471-1480. <https://doi.org/10.1111/cas.14828>